Exosomal transfer of miR-126 promotes the anti-tumour response in malignant mesothelioma: Role of miR-126 in cancer-stroma communication

Exosomal transfer of miR-126 promotes the anti-tumour response in malignant mesothelioma: Role of miR-126 in cancer-stroma communication

Federica Monaco[a], Simona Gaetani[a], Federica Alessandrini[b], Adriano Tagliabracci[b], Massimo Bracci[a], Matteo Valentino[a], Jiri Neuzil[c,d], Monica Amati[a], Massimo Bovenzi[e], Marco Tomasetti[a,*], Lory Santarelli[a,**]

[a] Department of Clinical and Molecular Sciences, Section of Experimental and Occupational Medicine, Polytechnic University of Marche, Via Tronto 10/A, 60126, Ancona, Italy
[b] Department of Biomedical Sciences and Public Health, Section of Legal Medicine, Polytechnic University of Marche, Via Tronto 10/A, 60126, Ancona, Italy
[c] Mitochondria, Apoptosis and Cancer Research Group, School of Medical Science, Griffith University, Southport, 4222, Qld, Australia
[d] Molecular Therapy Group, Institute of Biotechnology, Czech Academy of Sciences, Prague-West, 252 50, Czech Republic
[e] Department of Medical Sciences, University of Trieste, Trieste, Italy

ARTICLE INFO

Keywords:
Malignant mesothelioma
miR-126
Exosomes
Cancer stroma
miRNA-based therapy

ABSTRACT

MiR-126 has been shown to suppress malignant mesothelioma (MM) by targeting cancer-related genes without inducing toxicity or histopathological changes. Exosomes provide the opportunity to deliver therapeutic cargo to cancer stroma. Here, a tumour stromal model composed of endothelial cells (HUVECs), fibroblasts (IMR-90 cells), non-malignant mesothelial cells (Met-5A cells) and MM cells (H28 and MM-B1 cells) was used. The cells were treated with exosomes from HUVECs carrying endogenous (exo-HUVEC) and enriched miR-126 (exo-HUVEC$^{miR-126}$), and the uptake/turnover of exosomes; miR-126 distribution within the stroma; and effect of miR-126 on cell signalling, angiogenesis and cell proliferation were evaluated. Based on the sensitivity of MM cells to exo-HUVEC miR-126 treatment, miR-126 was distributed differently across stromal cells. The reduced miR-126 content in fibroblasts in favour of endothelial cells reduced angiogenesis and suppressed cell growth in an miR-126-sensitive environment. Conversely, the accumulation of miR-126 in fibroblasts and the reduced level of miR-126 in endothelial cells induced tube formation in an miR-126-resistant environment via VEGF/EGFL7 upregulation and IRS1-mediated cell proliferation. These findings suggest that transfer of miR-126 via HUVEC-derived exosomes represents a novel strategy to inhibit angiogenesis and cell growth in MM.

1. Introduction

Malignant mesothelioma (MM) is an aggressive tumour associated with occupational and environmental exposure to asbestos with limited therapeutic options. The therapy of choice for MM is treatment with cisplatin and pemetrexed; however, this treatment regime is mainly palliative and short-lasting with low efficacy [1]. Although immunotherapy has given new hope for the treatment of various types of cancer, it has thus far been disappointing in the case of MM [2]. New therapeutic strategies for MM are therefore warranted.

The altered expression of miRNAs in MM is linked to dysregulated metabolism and poor prognosis [3–5]. Therefore, miRNAs have become intriguing therapeutic targets for MM, and clinical trials investigating the effect of miRNA-based therapeutics are being launched [6–8]. Recently, a phase I trial evaluated the safety and biological activity of miR-16 in patients with recurrent MM [9]. MiR-16 administered in a minicell-based formulation was well tolerated by MM patients. In spite of its low toxicity, the proportion of patients that showed a response to this treatment was only 5%. Currently, the main barrier to implementing miRNA-based therapy is the lack of an effective delivery system to protect miRNAs from nuclease degradation, deliver them to the tumour stroma, and release them into target cancer cells.

Abbreviations: ADM, adrenomedullin; CAFs, cancer-associated fibroblasts; ECs, endothelial cells; EGFL7, epidermal growth factor like domain 7; EPCs, endothelial progenitor cells; ERK, extracellular signal-regulated kinase; FGF, fibroblast growth factor; FBs, fibroblasts; HGF, hepatocyte growth factor; HUVECs, human umbilical vein endothelial cells; IRS1, insulin receptor substrate 1; JNK, c-Jun NH2-terminal kinase; MM, malignant mesothelioma; TAFs, tumour-associated fibroblasts; VEGF, vascular endothelial growth factor

* Corresponding author. Department of Clinical and Molecular Sciences, Polytechnic University of Marche, Via Tronto 10/a, 60126, Ancona, Italy.
** Corresponding author. Department of Clinical and Molecular Sciences, Polytechnic University of Marche, Via Tronto 10/a, 60126, Ancona, Italy.
E-mail addresses: m.tomasetti@staff.univpm.it (M. Tomasetti), l.santarelli@univpm.it (L. Santarelli).

Accepted 5 August 2019

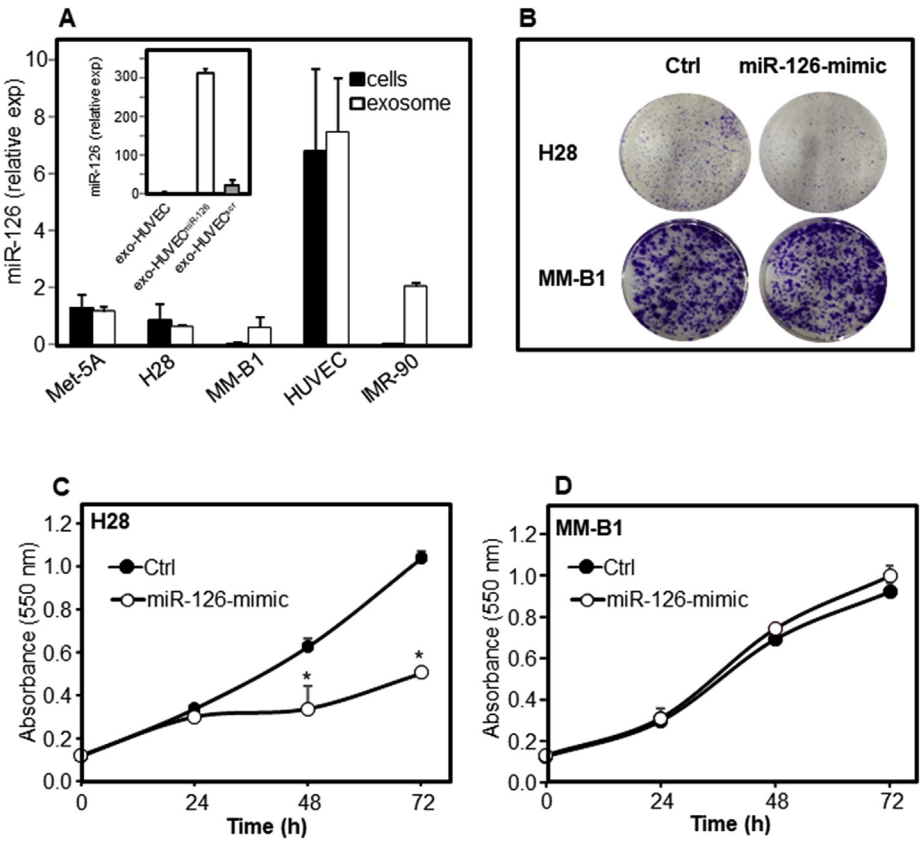

Fig. 1. MiR-126 levels in the cellular components and susceptibility of MM cells to miR-126 treatment. **A**) Cellular and exosomal levels of miR-126 in non-malignant mesothelial cells (Met-5A cells), sarcomatoid MM cells (H28 cells), biphasic MM cells (MM-B1 cells), endothelial cells (HUVECs) and fibroblasts (IMR-90 cells). The insert shows the levels of miR-126 in exosomes released by miR-126 and miRNA mimic scrambled control (scr)-transfected HUVECs. Colony formation assays in H28 and MM-B1 cells (**B**) and their proliferation curves (**C, D**) before and after miR-126 mimic treatment, respectively. The results are the mean values ± S.D.s of three experiments performed in duplicate. The symbol '*' denotes statistically significant differences between un-treated cells (Ctrl) and miR-126-mimic-treated cells, $p < 0.05$.

Exosomes are physiological carriers of miRNAs, and their involvement in cell-to-cell communication provides an opportunity to deliver therapeutic cargo directly into the cytoplasm of target cells. There is evidence of the effect of miR-126 as a tumour suppressor in MM in both cell culture and a xenograft model [4,10]. In the present study, the anticancer effect of miR-126 using exosomes as a delivery system was evaluated in an *in vitro* stromal model. Since miR-126 is highly expressed in endothelial cells (ECs), we used exosomes derived from human umbilical vein endothelial cells (HUVECs) to deliver and restore miR-126 in mesothelial cells and MM cells within three types of stromal environment, i.e., non-malignant, miR-126-sensitive and miR-126-resistant environments, and evaluate the anticancer effects of miR-126.

2. Materials and methods

2.1. Cell culture

Non-malignant (NM) mesothelial (Met-5A), sarcomatoid (H28), and biphasic (MSTO-211H) MM cell lines from the American Type Culture Collection (ATCC) and MM-B1 cells (biphasic) [11] were grown in RPMI-1640 medium. MPP89 epithelial cells obtained from the ATCC were maintained in Ham's F10 with 15% foetal bovine serum (FBS) and supplemented with glutamine (2 mM) and antibiotics. Human foetal lung fibroblasts (IMR-90) were obtained from the ATCC and grown in Dulbecco's modified Eagle's medium (DMEM). The RPMI medium and DMEM were supplemented with 10% FBS, 1% penicillin and 1% streptomycin (all Life Technologies). HUVECs obtained from Gibco (Life Technologies) were grown in Medium 200 (Life Technologies) with large vessel endothelial supplement (LVES; Life Technologies). All cells were cultured in a humidified incubator at 37 °C and in an atmosphere of 5% CO_2. The cells were periodically checked for the absence of mycoplasma contamination using the PCR mycoplasma test. Cell authentication was performed using a PowerPlex Fusion 6C system (Promega, Fitchburg, WI).

2.2. Transfection

MM cells were transiently transfected in exosome-depleted serum-containing medium with an miR-126 mimic, miRNA mimic scrambled control (100 nM, MISSION microRNA Mimic, Sigma), or antisense miR-126 (50 nM, anti-miR, Ambion), using High Perfect Transfection reagent (Qiagen) according to the manufacturer's instructions. After 72 h of incubation, exosomes enriched in miR-126, miRNA scrambled, or anti-miR were obtained.

2.3. Cell proliferation assay

Cell proliferation was assessed by the MTT assay. MM cells and their miR-126 mimic-transfected counterparts were incubated for 24, 48 and 72 h, following which cell viability was evaluated. Briefly, 10 µl of MTT (5 mg/ml in PBS; Sigma) was added to each well, and after 3 h incubation, the formed crystals were dissolved in isopropanol. The absorbance at 550 nm was read with an ELISA plate reader (Sunrise, Tecan).

2.4. Colony formation assay

H28 and MM-B1 cells and their miR-126 mimic-transfected counterparts were seeded in a 12-well plate at 500 cells per well. Colonies that formed after 10 days of incubation were fixed with formalin (4.0% v/v), stained with crystal violet (0.5% w/v) and counted using a stereomicroscope.

2.5. Exosome isolation and quantification

Exosomes were isolated and purified using differential centrifugations as previously described [12]. After isolation, the pellet was resuspended in PBS, treated with 0.1 mg/ml RNase A (Qiagen) for 30 min at 37 °C to remove miRNA contamination, and clarified using a

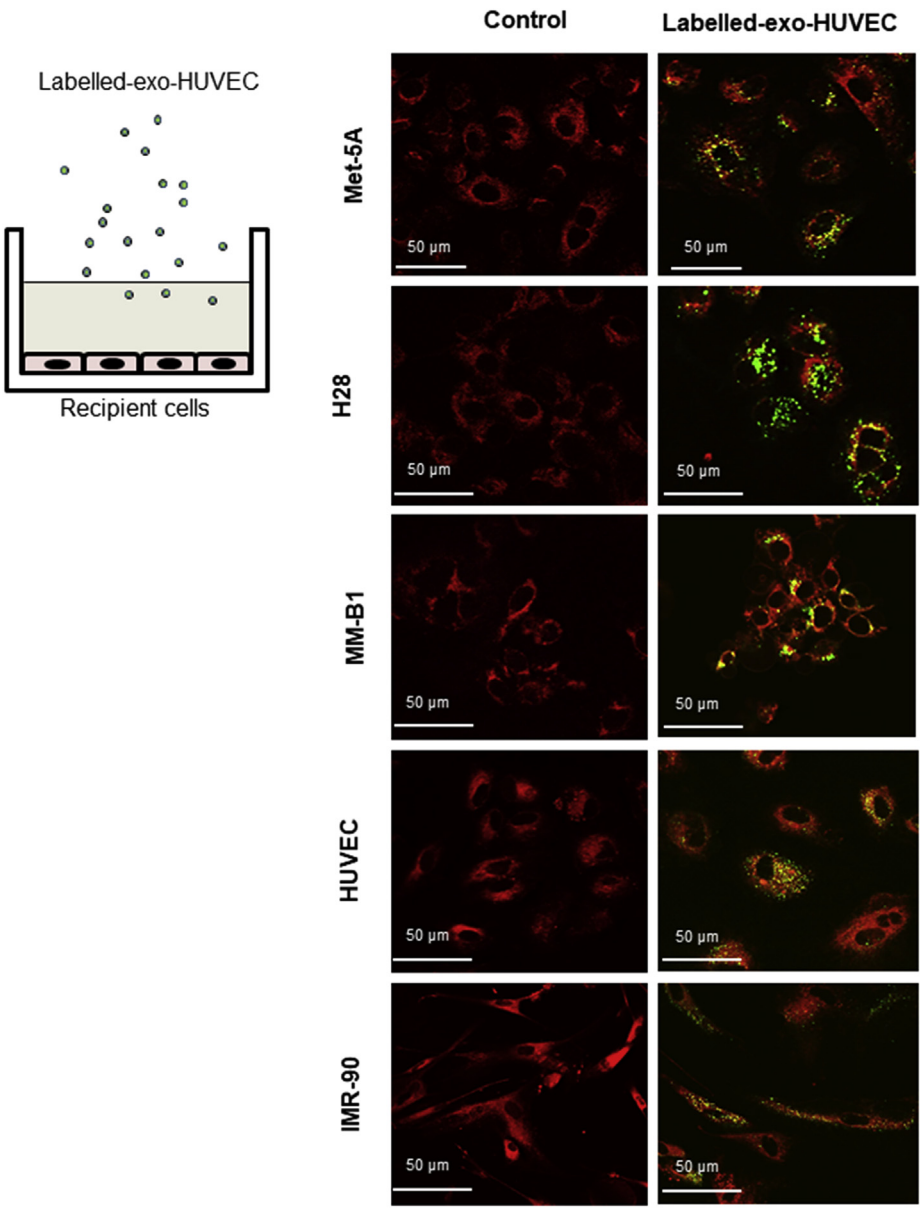

Fig. 2. Representative image showing HUVEC-derived exosome uptake by stromal cells. Met-5A, H28, MM-B1, and IMR-90 cells and HUVECs cultured in exosome-depleted serum were incubated with PKH67-labelled exosomes (exo-HUVEC, 50 μg/ml) for 6 h, as shown in the scheme (top left cartoon), and exosomal internalization was visualized by fluorescence microscopy (Zeiss, AxioCam MRc5). Mitochondria were stained with MitoTracker Red (100 nM) and used as a control. The scale bar indicates 50 μm. The images are representative of three independent experiments. (For interpretation of the references to colour in this figure legend, the reader is referred to the Web version of this article.)

0.22 μm filter before use. After treatment and filtration, the protein content of the purified exosomes was determined by the Bradford assay (Sigma). All ultracentrifugation steps were performed at 4 °C in a Beckton Dickinson ultracentrifuge fitted with the TLS-55 swing bucket rotor.

2.6. Exosome PKH67 labelling and uptake

Exosomes were labelled with the green fluorescence plasma membrane stain PKH67 (20 μM; Sigma) according to the manufacturer's instructions, and protein levels were measured using Bradford reagent. Cells (5×10^4) were seeded on coverslips in a 24-well plate and allowed to attach overnight, and PKH67-labelled exosomes (50 μg/ml) were added to the exosome-depleted culture medium. After 6 h of incubation, exosome uptake was assessed by confocal microscopy (Leica SP5). Mitochondria were stained with MitoTracker Red (100 nM; Molecular Probes). Alternatively, the cells were incubated with PKH67-labelled exosomes at increased concentrations in exosome-depleted cell culture medium, and exosome uptake was analysed over time by flow cytometry (FACSCalibur, BD).

2.7. Quantitative RT-PCR

Total cellular RNA was obtained using an RNeasy Mini Kit (Qiagen) according to the manufacturer's instructions. First-strand cDNAs were synthetized from the mRNAs by individual TaqMan miRNA Assay (Applied Biosystems, Life Technologies) according to the manufacturer's instructions. The qRT-PCR reactions were carried out using a TaqMan® Fast Advanced Master gene expression kit (Applied Biosystems, Life Technologies) and U6 for normalization. IRS1, VEGF, and EGFL7 first-strand cDNA was synthesized using a High-Capacity cDNA Reverse Transcription Kit (Life Technologies). qRT-PCR was performed using SYBR Select Master Mix (Life Technologies) with GAPDH as a housekeeping gene. The sequences of the primers used are listed in Supplementary Table 1.

To detect exosomal miR-126, RNA was extracted from exosomes (20 μg protein), and miR-126 expression was evaluated as previously described [3].

2.8. Tri-culture model

Tri-culture was performed by layering fibroblasts (IMR-90) and

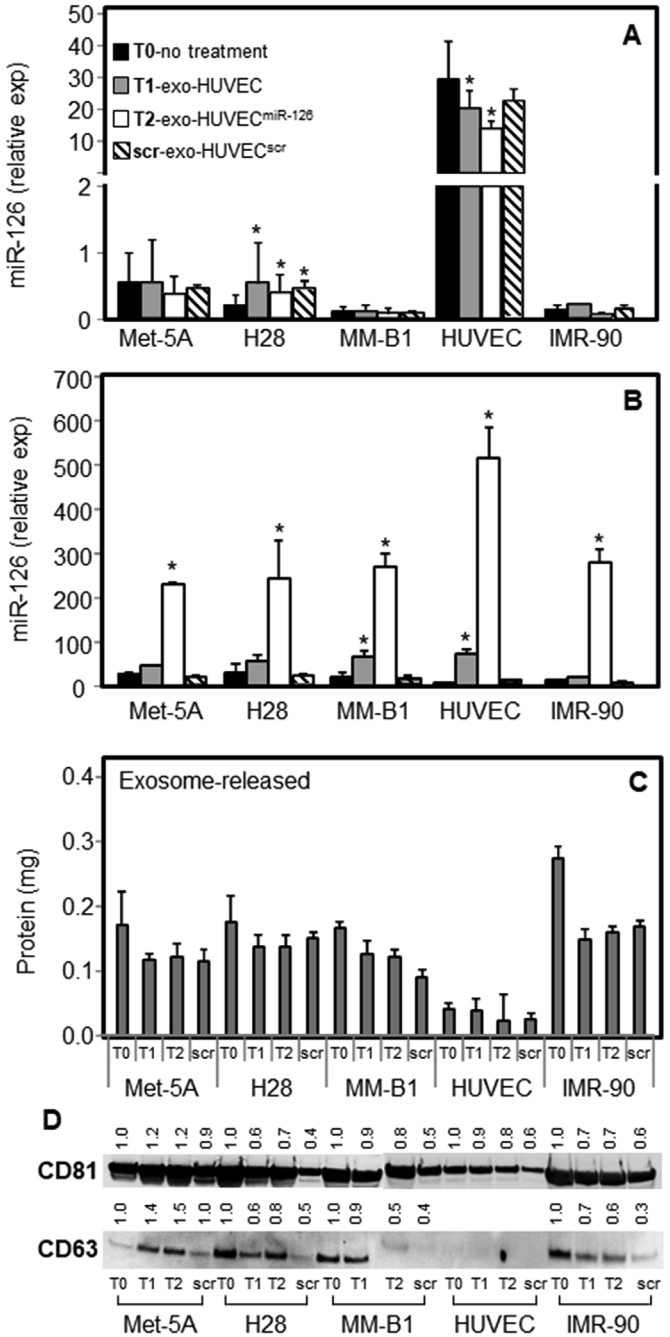

Fig. 3. Exosomal transfer of miR-126 between cells and exosomes. Stromal cells (Met-5A, H28, MM-B1, and IMR-90 cells and HUVECs) were treated with HUVEC-derived exosomes (T1), exosome-enriched miR-126 (T2), or exosome-enriched miRNA scrambled control (scr), and after 24 h of incubation, the levels of miR-126 in cells (**A**) and exosomes (**B**) were evaluated. The released exosomes were quantified by detecting exosomal protein using the Bradford assay **(C)**, and CD81 and CD63 levels were assessed by Western blot analysis, and the results expressed as fold change respect to the T0 **(D)**. The results are the mean values ± S.D.s of three experiments performed in duplicate. Comparisons among treatments were performed by ANOVA with Tukey's post hoc analysis. The symbol '*' denotes statistically significant differences between un-treated cells (T0) and exo-miR-126-treated cells (T1,T2 and scr), $p < 0.05$.

endothelial cells (HUVECs) on two opposite surfaces of Transwell inserts, with NM (Met-5A) or MM (H28, MPP89, MSTO-211H or MM-B1) cells cultured at the bottom of the plate. HUVEC-derived exosomes and miR-126- or anti-miR-enriched exosomes (20 μg/ml) were added to the upper chamber of the tri-culture system, and the cells were collected after 24 or 48 h of incubation.

2.9. Angiogenetic activity assessment

Angiogenesis was determined by evaluating the formation of capillary-like structures in a three-dimensional setting. Tube formation was assessed by incubating (16 h) HUVEC-derived exosomes and miR-126- or anti-miR-enriched exosomes (20 μg/ml) with Met-5A, H28, MPP89, MSTO-211H or MM-B1 cells in the tri-culture system with IMR-90 cells using 3-μm Transwell inserts. After incubation, polygonal structures made up of a network of endothelial cell capillaries were established, and images were captured at 10 × magnification using an AxioCam MRc5 optical microscope (Zeiss). Tube formation was estimated by counting the number of complete capillaries connecting individual points of the polygonal structures. Three fields in the central area in each well were chosen randomly.

2.10. Ki-67 proliferation assay

Met-5A, H28, MPP89, MSTO-211H or MM-B1 cells were seeded on coverslips in a 24-well plate in the tri-culture system and treated with HUVEC-derived exosomes and miR-126- or anti-miR-enriched exosomes (20 μg/ml) for 48 h. The cells were then fixed (4% formalin for 30 min at 4 °C) and permeabilized (0.05% saponin and 2% FBS in PBS for 30 min at 4 °C). Next, the cells were incubated overnight at 4 °C with a primary antibody against Ki-67 (1:200; DAKO) and a FITC-conjugated secondary IgG (Sigma). Ki-67-positive cells were evaluated by fluorescence microscopy (Zeiss; AxioCam MRc5, magnification 60 ×). The proliferation index was expressed as the percentage of Ki-67-positive cells.

2.11. Western blot analysis

Cells or exosomes (10 μg of protein or 20 μl of exosome suspension) were lysed in RIPA buffer containing Na_3VO_4 (1 mM) and protease inhibitors (1 μg/ml). Protein concentration was assessed by the Bradford assay. The cell and exosome lysates were separated using 4–12% SDS-PAGE (Life Technologies) and transferred onto a nitrocellulose membrane (Protran). After blocking with 5% non-fat milk in PBS-Tween (0.1%), the membranes were incubated overnight at 4 °C with primary antibodies against IRS1 (Bethyl), phospho-p38 MAPK, p38 MAPK, phospho-AKT and AKT (all Cell Signalling). β-Actin (Cell Signalling) was used as a loading control. Anti-CD81 and anti-CD63 IgG (generously provided by Prof. Fabio Malavasi, University of Torino, Italy) were used to detect exosomes. After incubation with HRP-conjugated secondary IgG (Cell Signalling), the blots were developed using ECL (Pierce). The band intensities were visualized and quantified with ChemiDoc using Quantity One software (Bio-Rad Laboratories).

2.12. Statistical analysis

Data are presented as means ± standard deviations (SDs). Comparisons between and among groups of data were determined using Student's t-test and one-way analysis of variance (ANOVA) with Tukey's post hoc analysis. A p-value ≤ 0.05 indicated statistical significance. All statistical analyses were performed using SPSS software.

3. Results

3.1. MiR-126 level in cellular stroma components and MM cell response to miR-126 treatment

The levels of miR-126 in MM cellular stroma components, such as NM or MM cells (mesothelial Met-5A cells, sarcomatoid H28 cells, biphasic MM-B1 cells), IMR-90 cells and HUVECs, were evaluated. Among these cells, HUVECs showed the highest miR-126 content in

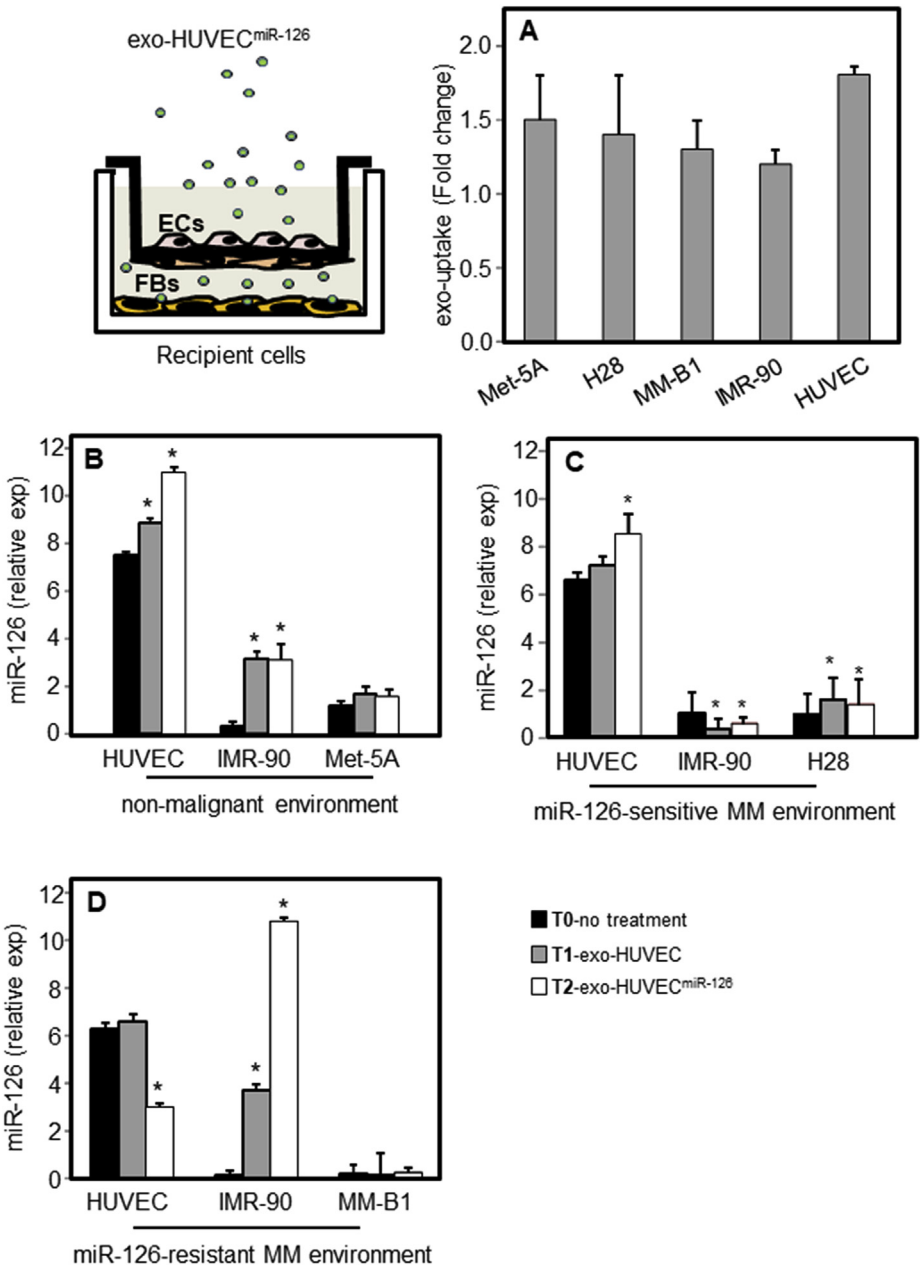

Fig. 4. Exosomal uptake and exosomal miR-126 transfer in the stromal model. The stromal model is represented in the scheme (top left cartoon). Exosomal uptake (**A**) and miR-126 levels in cells (recipient cells) in the stromal environments of a non-malignant environment (**B**), an miR-126-sensitive MM environment (**C**), and an miR-126-resistant MM environment (**D**) following no treatment (T0), exosome-endogenous miR-126 treatment (T1), and exosome-enriched miR-126 treatment (T2). The results are the mean values ± S.D.s of three experiments performed in duplicate. The symbol '*' denotes statistically significant differences between un-treated cells (T0) and exo-HUVEC-treated cells (T1 and T2), $p < 0.05$.

both the cellular and exosomal compartments (Fig. 1A). HUVECs transfected with the miR-126 mimic exhibited further increased exosomal miR-126 content. The transfection of HUVECs with a nonspecific miRNA mimic scrambled control did not affect the exosomal miR-126 content (Fig. 1A, insert).

Next, we evaluated the sensitivity of MM cells to the effects induced by miR-126. H28 and MM-B1 cells were treated with the miR-126 mimic and subjected to cell proliferation and colony formation assays. As shown in Fig. 1B–D, miR-126 inhibited the growth of H28 cells (miR-126-sensitive cells) but had no effect on MM-B1 cells (miR-126-resistant cells).

3.2. Uptake of HUVEC-derived exosomes and the transfer of miR-126 in stromal cells

Given that HUVECs released exosomes rich in miR-126 and miR-126 transfection further increased the miR-126 level in HUVECs, we used exosomes from control HUVECs as an endogenous delivery system for miR-126 (exo-HUVEC). The exosomal uptake in all cellular components of the stromal model was evaluated. All cells were able to internalize the exosomes, as visualized by punctuate green fluorescence (Fig. 2). Next, the kinetics of exosomal uptake were evaluated by quantitative flow cytometry assay. PKH67-labelled exosomes (exo-HUVEC) were administered at an increasing amount, and exosomal uptake by stroma recipient cells was evaluated over time. As shown in Supplementary Fig. 1, the uptake of exosomes at 100 μg/ml exosome protein was linear for up to 360 min. Stromal cells took up labelled exosomes in a time- and concentration-dependent manner (Supplementary Fig. 1, insert). As shown by the kinetic analysis, exosomal uptake was rapid in MM-B1 cells and HUVECs (Supplementary Fig. 1, bottom right image). Next, we evaluated the exosomal transfer of miR-126 between cells and the release of miR-126 into the medium. Cells were treated with exo-HUVEC (T1), exo-HUVEC miR-126 enriched (T2), or exo-HUVEC scrambled (exo-HUVEC^{scr}), and the miR-126 contents in both cells and exosomes released into the medium were detected. MiR-126 was found to accumulate in H28 cells, while miR-126 levels decreased in HUVECs following treatment (Fig. 3A). The effects of exo-HUVEC^{scr} treatment resembled those of T1 treatment (exo-HUVEC) in stromal cells, while the

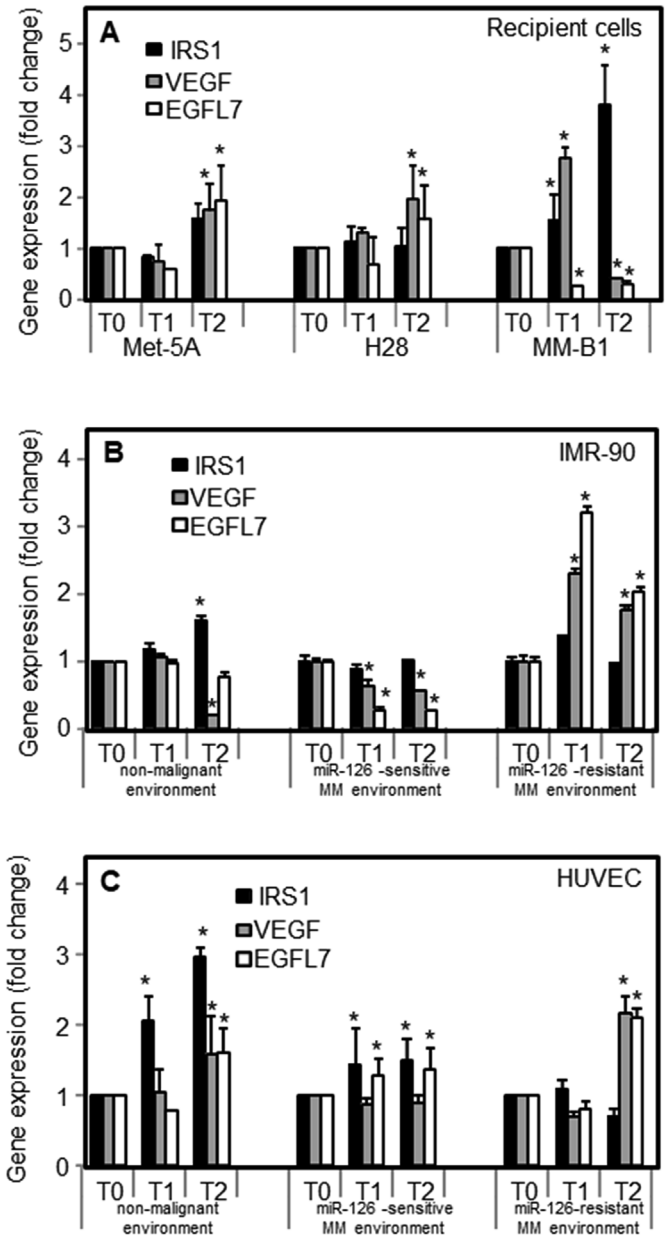

Fig. 5. Modulation of miR-126 target expression by exosome-delivered miR-126 in the stroma model. **A)** IRS1, VEGF, and EGFL7 gene expression was evaluated in recipient Met-5A cells (non-malignant environment), H28 cells (miR-126-sensitive MM environment) and MM-B1 cells (miR-126-resistant MM environment) or IMR-90 cells (**B**) and HUVECs (**C**) within the three MM environments. The results are the mean values ± S.D.s of three experiments performed in duplicate. The symbol '*' denotes statistically significant differences between un-treated cells (T0) and exo-HUVEC-treated cells (T1 and T2), $p < 0.05$.

miR-126 content in exosomes released by the cells after treatment was decreased (Fig. 3A and B). Although exosome release was decreased by treatment (Fig. 3C and D), the released exosomes were enriched in miR-126 (Fig. 3B).

3.3. Exosome uptake and exo-HUVEC miR-126 distribution in the stromal model

To investigate the interactions between cancer cells and cancer-associated cells within the tumour microenvironment, an *in vitro* stromal model was used. By stratifying ECs (HUVECs) and fibroblasts (IMR-90 cells) on the upper and lower surfaces of a Transwell insert and normal or MM cells (miR-126-sensitive and miR-126-resistant cells, respectively) on the bottom of the well in which the insert was placed (Fig. 4, top left cartoon), three microenvironments were obtained: (*i*) non-malignant, (*ii*) miR-126-sensitive and (*iii*) miR-126-resistant environments. Next, after turning the cells from the insert to the bottom of the well (recipient cells), both exosomal uptake and miR-126 content after exo-HUVEC treatments (T1 and T2) in each cellular component were evaluated. Exosome uptake was observed in all cellular components (Fig. 4A). Treatment in the non-malignant environment increased the level of miR-126 in IMR-90 cells and HUVECs without changing the miR-126 level in Met-5A cells (Fig. 4B). An increased level of miR-126 in H28 cells and HUVECs associated with a reduction in miR-126 in IMR-90 cells was found in the miR-126-sensitive MM environment following treatment (Fig. 4C). Conversely, in the miR-126-resistant MM environment, treatment increased the level of miR-126 in IMR-90 cells, which was associated with a reduction in miR-126 content in both MM-B1 cells and HUVECs (Fig. 4D). The distribution of miR-126 among the cells in the three environments was also evaluated (Supplementary Fig. 2). MiR-126 accumulated in fibroblasts in the non-malignant environment after treatment. In the miR-126-sensitive MM environment, miR-126 was transferred following treatment and accumulated in H28 cells and HUVECs. Conversely, in the miR-126-resistant MM environment, miR-126 introduced by treatment was sequestered by fibroblasts (36–77%), thus reducing the miR-126 level in both MM-B1 cells and HUVECs.

Given that the microenvironment affected the miR-126 distribution among the cells, we next evaluated the modulation of miR-126 target genes following exo-HUVEC treatment. The following three miR-126 targets involved in angiogenesis and cell growth were evaluated: insulin receptor substrate 1 (IRS1), vascular endothelial growth factor (VEGF) and EGF-like domain 7 (EGFL7). The treatments induced the expression of VEGF and EGFL7 in Met-5A and H28 cells and upregulated IRS1 in MM-B1 cells (Fig. 5A). VEGF and EGFL7 were found to be downregulated in IMR-90 cells in the miR-126-sensitive MM environment. In contrast, treatment induced VEGF and EGFL7 expression in both IMR-90 cells and HUVECs in the miR-126-resistant MM environment (Fig. 5B and C).

3.4. Exo-HUVEC miR-126 treatment modulated angiogenesis and cell growth in the stromal model

The increased expression of VEGF and EGFL7 in IMR-90 cells and HUVECs in the miR-126-resistant MM environment following exo-HUVEC treatment contributed to angiogenesis induction in the stromal model. In contrast, treatment with exosomes inhibited vessel formation in the miR-126-sensitive MM environment. Angiogenesis was slightly inhibited in the non-malignant environment following treatment. These effects were reversed by blocking the function of miR-126 using antisense miR126 (anti-miR), which further confirmed the involvement of miR-126 in these effects (Fig. 6A). Notably, these results were inverted in a co-culture system without fibroblasts (IMR-90 cells), in which exo-HUVEC treatment inhibited vessel formation in the miR-126-resistant MM environment and induced angiogenesis in the miR-126-sensitive environment. This finding suggests a role for fibroblasts in the modulation of angiogenesis (Fig. 6B). However, when miR-126-sensitive (H28) and miR-126-resistant (MM-B1) MM cells were grown together, angiogenesis was inhibited by exo-HUVEC treatment (Fig. 6C).

The IRS1 protein, a direct target of miR-126, is involved in tumour suppression [10,13]. Therefore, the impact of exosome treatment on the modulation of IRS1 signalling was evaluated in non-malignant Met-5A and MM cells (H28 and MM-B1) in the tri-culture stromal model. Exo-HUVEC treatment markedly inhibited IRS1 expression, which was associated with the reduced expression of downstream AKT and p38 targets in the miR-126-sensitive MM environment. Conversely, the increased expression of IRS1 observed in the miR-126-resistant

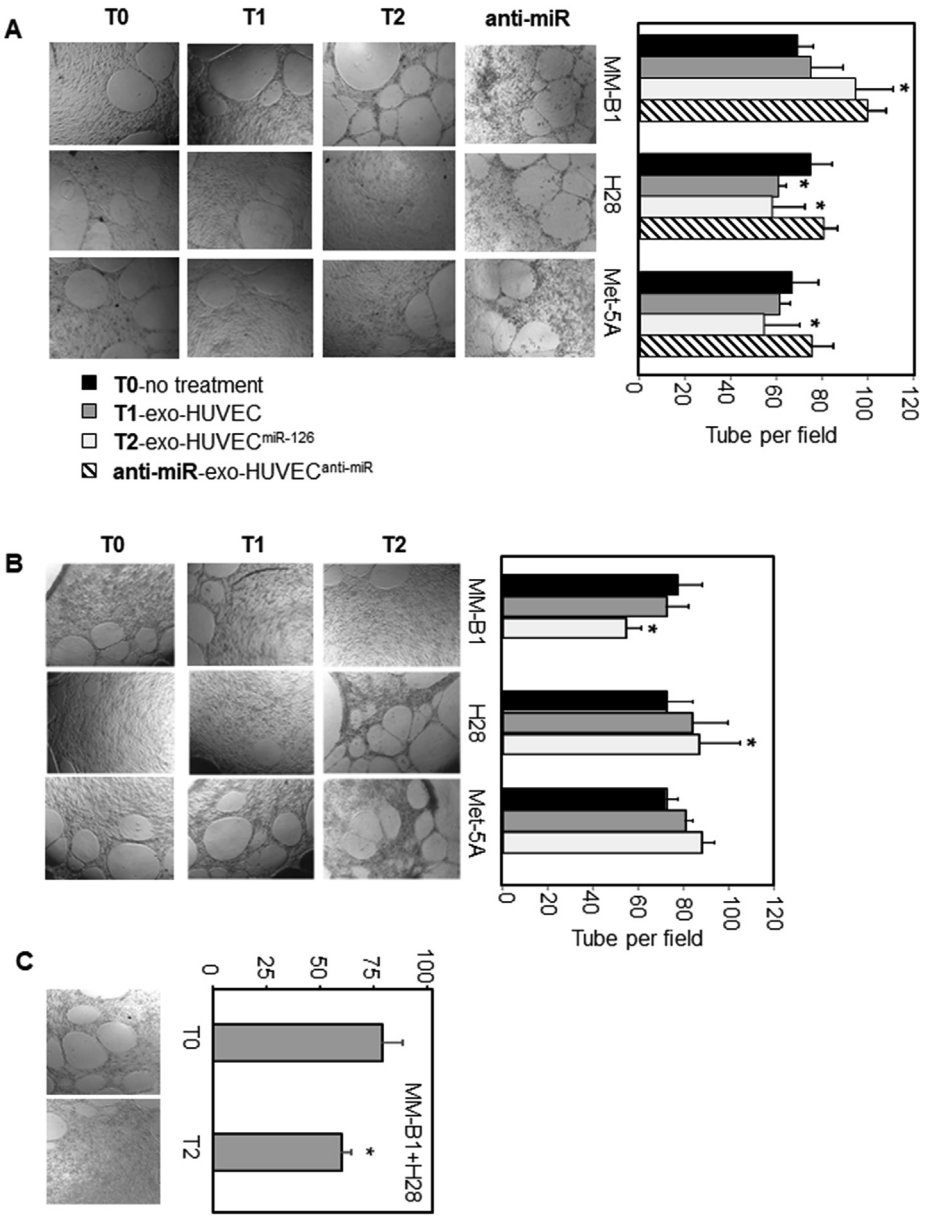

Fig. 6. Regulation of angiogenesis by exosome-delivered miR-126 in the stromal model. Angiogenesis was evaluated via tube formation in a tri-culture model in which non-malignant mesothelial cells (Met-5A cells) or MM cells (H28 and MM-B1 cells) and fibroblasts (IMR-90 cells) were grown on the upper and lower surface of a Transwell insert, respectively, with endothelial cells (HUVECs) grown at the bottom of the well. **A**) MM-B1 cells (miR-126-resistant MM environment), H28 cells (miR-126-sensitive MM environment) and Met-5A cells (non-malignant environment) were treated with exo-miR-126 (T1 and T2) or exo-HUVEC$^{anti\text{-}miR}$, and tube formation was visualized and quantified. **B**) MM-B1 and H28 cells cultured in the stromal environment without fibroblasts were treated with exo-HUVEC$^{miR-126}$ (T2), and tube formation was visualized and quantified. **C**) H28 and MM-B1 cells were co-cultured in the stroma model, and vessel formation was evaluated after exo-HUVEC$^{miR-126}$ (T2) treatment. The images are representative of three independent experiments performed in duplicate. The symbol '*' denotes statistically significant differences between un-treated cells (T0) and exo-HUVEC-treated cells (T1, T2 and anti-miR), $p < 0.05$.

environment in response to treatment did not affect the signalling pathway (Fig. 7). Cell proliferation was also evaluated in the tri-culture model after incubation with exo-HUVEC. As shown in Fig. 8, the percentage of Ki-67-positive cells was significantly decreased in the miR-126-sensitive MM environment after treatment, which was reversed by anti-miR. No Ki-67-positive cells were detected in MM-B1 cells. The relationship between miR-126 stromal distribution, angiogenesis and cell growth was further confirmed in two other MM cell lines with epithelial (MPP89) and biphasic (MSTO-211H) phenotypes, showing the pronounced inhibition of cell growth and angiogenesis in miR-126-responsive MSTO-211H cells (Supplementary Fig. 3).

4. Discussion

Based on the results in this report, we propose exosomes as carriers for the delivery of miR-126, an miRNA previously found to suppress MM tumour formation in mice. An *in vitro* study was performed to evaluate the impact of miR-126 delivered by exosomes on cell-to-cell communication within the stroma of MM. Exosomes from endothelial cells were used as a natural carrier of miR-126 (cf Fig. 1). Therefore, exosome-delivered endogenous miR-126 and miR-126 enriched by mimic transfection (exo-HUVEC$^{miR-126}$) were used to treat MM cells. The cells responded differently to the treatments. The cancer stroma consists of a heterogeneous group of cells whose growth and progression greatly depend on reciprocal interactions between genetically altered neoplastic cells and the non-neoplastic microenvironment [14,15]. All cellular components of the 'stroma' took up exo-miR-126 in a dose- and time-dependent manner and released exosomes enriched in miR-126 into the microenvironment; these exosomes may be internalised by the cells themselves or other cellular components of the environment (cf Figs. 2 and 3). A negative feedback mechanism of exosome release has been observed (Fig. 3). Exosomes introduced by exo-HUVEC treatments can suppress the further release of exosomes from the cells, as previously reported [16,17].

In a tri-culture system, miR-126 was introduced and distributed among the cells via autocrine and paracrine mechanisms. Therefore, by culturing fibroblasts and ECs with Met-5A, H28 and MM-B1 cells, three environments were formed: non-malignant, miR-126-sensitive and miR-126-resistant MM environments. Consistent with the formation of individual environments, miR-126 delivered by exosomes was distributed

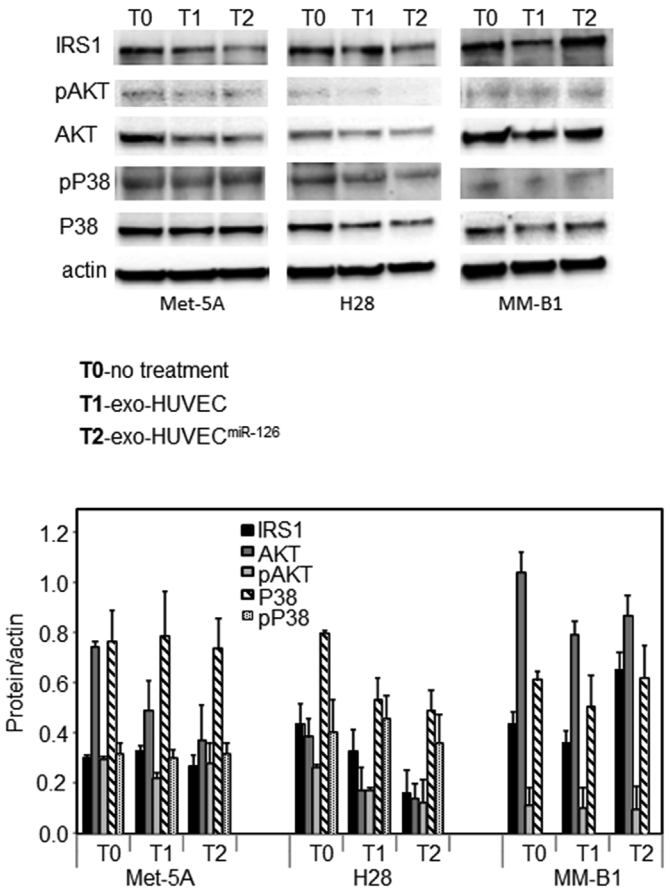

Fig. 7. Activation of IRS1 signalling by exosome-delivered miR-126 in the stromal model. Non-malignant mesothelial cells (Met-5A cells) or MM cells (H28 and MM-B1 cells) grown in the tri-culture system with fibroblasts (IMR-90) and endothelial cells (HUVECs) were treated with exo-HUVEC (T1) or exo-HUVEC$^{miR-126}$ (T2) (20 μg/ml), and the expression of IRS1, pAKT, AKT, pP38, and P38 was evaluated after 2 days of incubation. Band densities were related to the level of actin (bottom panel). The images are representative of three independent experiments performed in duplicate.

differently across the cells, thereby affecting angiogenesis and cell growth. For instance, exo-HUVEC miR-126 treatment induced miR-126 upregulation in ECs in the miR-126-sensitive MM environment. The downregulation of miR-126 in ECs and high miR-126 levels in fibroblasts were found in the miR-126-resistant MM environment (cf Fig. 4; Sup. 2). In the latter case, a shift of the miR-126 content from endothelial cells to fibroblasts induced tube formation, which was suppressed in the culture system lacking fibroblasts, suggesting the role of these cells in cancer-stroma cross-talk (cf Fig. 6). The induction of angiogenesis was related to high levels of EGFL7 and VEGF. Fibroblasts contributed to blood vessel abnormalities by altering their secretion of various pro- and anti-angiogenic factors [18]. Among these factors, EGFL7 is an endothelial cell-derived factor involved in regulating the spatial arrangement of cells during vascular tube formation and remodelling [19].

Although functional EGFL7 protein is regulated by miR-126 expression, whether EGFL7 protein and microRNA act in synergy or antagonistically is unclear. The infiltration of cancer-associated fibroblasts (CAFs) has been found in MM specimens, and lung fibroblast-conditioned medium promoted MM cell growth and migration via the production of fibronectin and hepatocyte growth factor (HGF) [20]. Fibronectin acts as a chemoattractant for fibroblasts, ECs and cancer cells; HGF, which is expressed at high levels in MM patients [21], likely plays an important role in tumour progression. Similarly, the fibroblast growth factor (FGF) is a potent driver of malignancy in MM that can be regulated by the miR-15/16 family [22].

Breast cancer cells mixed with CAFs enhanced tumour formation by angiogenesis via adrenomedullin (ADM) secretion [23]. Cross-talk between cervical cancer cells and fibroblasts has been reported to induce the downregulation of miR-126 in HUVECs with a consequent increase in tube formation. The pro-angiogenetic ADM was identified as a target inhibited by miR-126 [24]. Therefore, we postulate that the exosome-induced upregulation of miR-126 in endothelial cells inhibits ADM expression, thus inhibiting angiogenesis. We demonstrated that cross-talk between MM cells and fibroblasts modulated angiogenesis, which was dependent on the response of MM cells to miR-126 treatment. However, in a heterogeneous cell environment in which cells respond differently to the miR-126 treatment, the inhibitory effect of miR-126 on angiogenesis in miR-126-sensitive MM cells was greater than that in the miR-126-resistant cells, indicating the efficacy of the treatments.

Various studies have shown that inhibition of IRS1 results in the downregulation or inhibition of angiogenesis [24–27] and that IRS1 expression and activation are associated with the MM phenotype [28]. Here, we found that exo-HUVEC miR-126 treatment affected IRS1 signalling by modulating the AKT and MAPK pathways downstream of IRS1 (cf Fig. 7). MAPK proteins include extracellular signal-regulated kinase (ERK), p38, and the c-Jun NH2-terminal kinase (JNK). The signalling pathways associated with these proteins regulate a variety of cellular activities, including proliferation, differentiation, survival, and death [29]. Inhibition of the IRS1 pathway with the consequent arrest of cell growth was observed in the miR-126-sensitive MM environment after exo-HUVEC miR-126 treatment. Conversely, MM cells resistant to miR-126 showed the increased expression of IRS1, which was associated with increased cell proliferation. Taken together, these data suggest that cross-talk between MM cells and components of the stroma, such as fibroblasts and ECs, modulates miR-126 distribution within the stromal environment following exo-HUVEC miR-126 treatment. The reduced miR-126 content in fibroblasts in favour of ECs inhibited both angiogenesis and cell growth. In contrast, the accumulation of miR-126 in fibroblasts and the reduced level of miR-126 in ECs induced tube formation via VEGF/EGFL7 upregulation and IRS1-mediated cell proliferation. Consistently, exosomes from HUVECs have been proposed to alleviate ischaemic injury [30,31], and miR-126-loaded exosomes obtained from marrow-derived endothelial progenitor cells were used to treat thrombotic events in an animal model [32]. Therefore, the transfer of miR-126 via HUVEC-derived exosomes may represent a novel strategy to inhibit angiogenesis and the proliferation of MM with translational consequences.

Author contributions

Federica Monaco and Marco Tomasetti: conceptualization and data analysis; Simona Gaetani and Federica Alessandrini; methodology; Adriano Tagliabracci, Massimo Bracci, Matteo Valentino and Monica Amati: validation and visualization, Jiri Neuzil, Massimo Bovenzi, and Lory Santarelli: project administration, funding acquisition, supervision; Jiri Neuzil and Marco Tomasetti: manuscript writing and revision.

Conflicts of interest statement

There is no conflict of interest.

Acknowledgements

This work was supported by grant n. 0016902/P (11/09/2018) from Region Friuli Venezia Giulia (Italy) and Czech Health Research Council grant (16-31704A) to Jiri Neuzil.

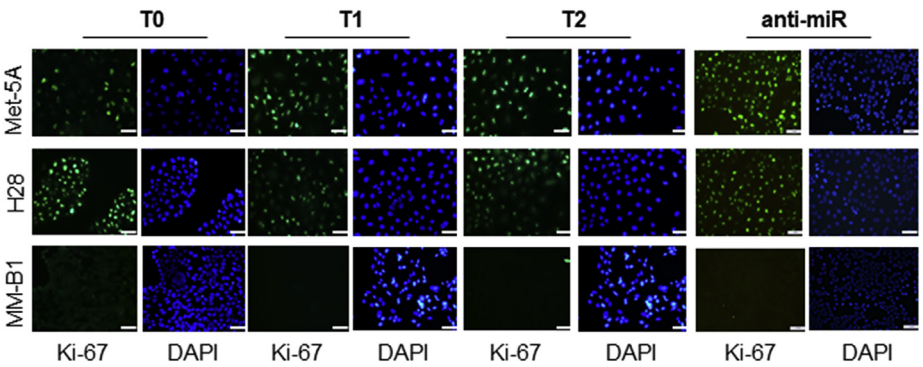

Fig. 8. Modulation of proliferation by exosome-delivered miR-126 in the stroma model determined by Ki-67 staining. Non-malignant mesothelial cells (Met-5A cells) or MM cells (H28 and MM-B1 cells) grown in the tri-culture system with fibroblasts (IMR-90 cells) and endothelial cells (HUVECs) were treated with exo-HUVEC (T1), exo-HUVEC$^{miR-126}$ (T2) or exo-HUVEC$^{anti-miR}$ (20 μg/ml), and evaluated for Ki-67-positive cells (%) after 2 days of incubation. The images are representative of three independent experiments performed in duplicate. The scale bar indicates 50 μm. The symbol "*" denotes statistically significant differences between un-treated cells (T0) and exo-miR-126-treated cells (T1, T2 and anti-miR), $p < 0.05$.

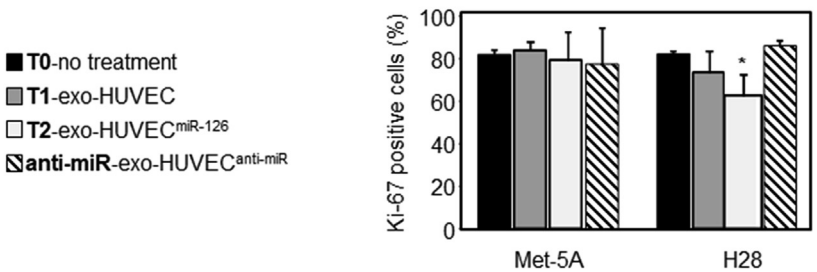

References

[1] L. Mutti, T. Peikert, B.W.S. Robinson, A. Scherpereel, A.S. Tsao, M. de Perrot, G.A. Woodard, D.M. Jablons, J. Wiens, F.R. Hirsch, H. Yang, M. Carbone, A. Thomas, R. Hassan, Scientific advances and new frontiers in mesothelioma therapeutics, J. Thorac. Oncol. 13 (2018) 1269–1283.

[2] L. Ye, S. Ma, B.W. Robinson, J. Creaney, Immunotherapy strategies for mesothelioma - the role of tumor specific neoantigens in a new era of precision medicine expert, Rev. Respir. Med. (2018) 1–12.

[3] M. Tomasetti, S. Staffolani, L. Nocchi, J. Neuzil, E. Strafella, N. Manzella, L. Mariotti, M. Bracci, M. Valentino, M. Amati, L. Santarelli, Clinical significance of circulating miR-126 quantification in malignant mesothelioma patients, Clin. Biochem. 45 (2012) 575–581.

[4] M. Tomasetti, L. Nocchi, S. Staffolani, N. Manzella, M. Amati, J. Goodwin, K. Kluckova, M. Nguyen, E. Strafella, M. Bajzikova, M. Peterka, S. Lettlova, J. Truksa, W. Lee, L.F. Dong, L. Santarelli, J. Neuzil, MicroRNA-126 suppresses mesothelioma malignancy by targeting IRS1 and interfering with the mitochondrial function, Antioxidants Redox Signal. 21 (2014) 2109–2125.

[5] C. De Santi, O. Melaiu, A. Bonotti, L. Cascione, G. Di Leva, R. Foddis, A. Cristaudo, M. Lucchi, M. Mora, A. Truini, A. Tironi, B. Murer, R. Boldorini, M. Cipollini, F. Gemignani, P. Gasparini, L. Mutti, S. Landi, Deregulation of miRNAs in malignant pleural mesothelioma is associated with prognosis and suggests an alteration of cell metabolism, Sci. Rep. 7 (2017) 3140.

[6] A. Bhardwaj, S. Singh, A.P. Singh, MicroRNA-based cancer therapeutics, Big Hope from Small RNAs Molecular and Cellular Pharmacology, 2 2010, pp. 213–219.

[7] M.Y. Shah, G.A. Calin, MicroRNAs as therapeutic targets in human cancers, Wiley Interdisciplinary Reviews, RNA, 5 2014, pp. 537–548.

[8] R. Gambari, E. Brognara, D.A. Spandidos, E. Fabbri, Targeting oncomiRNAs and mimicking tumor suppressor miRNAs: new trends in the development of miRNA therapeutic strategies in oncology, Int. J. Oncol. 49 (2016) 5–32.

[9] N. van Zandwijk, N. Pavlakis, S.C. Kao, A. Linton, M.J. Boyer, S. Clarke, Y. Huynh, A. Chrzanowska, M.J. Fulham, D.L. Bailey, W.A. Cooper, L. Kritharides, L. Ridley, S.T. Pattison, J. MacDiarmid, H. Brahmbhatt, G. Reid, Safety and activity of microRNA-loaded minicells in patients with recurrent malignant pleural mesothelioma: a first-in-man, phase 1, open-label, dose-escalation study, Lancet Oncol. 18 (2017) 1386–1396.

[10] M. Tomasetti, F. Monaco, N. Manzella, J. Rohlena, K. Rohlenova, S. Staffolani, S. Gaetani, V. Ciarapica, M. Amati, M. Bracci, M. Valentino, J. Goodwin, M. Nguyen, J. Truksa, M. Sobol, P. Hozak, L.F. Dong, L. Santarelli, J. Neuzil, MicroRNA-126 induces autophagy by altering cell metabolism in malignant mesothelioma, Oncotarget 7 (2016) 36338–36352.

[11] M. Tomasetti, M.R. Rippo, R. Alleva, S. Moretti, L. Andera, J. Neuzil, A. Procopio, Alpha-tocopheryl succinate and TRAIL selectively synergise in induction of apoptosis in human malignant mesothelioma cells, Br. J. Canc. 90 (2004) 1644–1653.

[12] F. Grimolizzi, F. Monaco, F. Leoni, M. Bracci, S. Staffolani, C. Bersaglieri, S. Gaetani, M. Valentino, M. Amati, C. Rubini, F. Saccucci, J. Neuzil, M. Tomasetti, L. Santarelli Exosomal, miR-126 as a circulating biomarker in non-small-cell lung cancer regulating cancer progression, Sci. Rep. 7 (2017) 15277.

[13] Y. Sakurai, N. Kubota, I. Takamoto, A. Obata, M. Iwamoto, T. Hayashi, M. Aihara, T. Kubota, H. Nishihara, T. Kadowaki, Role of insulin receptor substrates in the progression of hepatocellular carcinoma, Sci. Rep. 7 (2017) 5387.

[14] J. Minnema-Luiting, H. Vroman, J. Aerts, R. Cornelissen, Heterogeneity in immune cell content in malignant pleural mesothelioma, Int. J. Mol. Sci. 19 (2018) 1041.

[15] D. Thomas, P. Radhakrishnan, Tumor-stromal crosstalk in pancreatic cancer and tissue fibrosis Mol, Cancer 18 (2019) 14.

[16] A. Riches, E. Campbell, E. Borger, S. Powis, Regulation of exosome release from mammary epithelial and breast cancer cells - a new regulatory pathway, Eur. J. Cancer 50 (2014) 1025–1034.

[17] M. Moloudizargari, M.H. Asghari, M. Abdollahi, Modifying exosome release in cancer therapy: how can it help? Pharmacol. Res. 134 (2018) 246–256.

[18] F.G. Kugeratski, S.J. Atkinson, L.J. Neilson, S. Lilla, J.R.P. Knight, J. Serneels, A. Juin, S. Ismail, D.M. Bryant, E.K. Markert, L.M. Machesky, M. Mazzone, O.J. Sansom, S. Zanivan, Hypoxic cancer-associated fibroblasts increase NCBP2-AS2/HIAR to promote endothelial sprouting through enhanced VEGF signaling, Sci. Signal. 12 (2019).

[19] I. Nikolic, K.H. Plate, M.H.H. Schmidt EGFL7 meets miRNA-126: an angiogenesis alliance, Angiogenes Res. 2 (2010) 9.

[20] N. Kanaji, N. Kita, N. Kadowaki, S. Bandoh, Fibronectin and hepatocyte growth factor produced by lung fibroblasts augment migration and invasion of malignant pleural mesothelioma cells, Anticancer Res. 37 (2017) 2393–2400.

[21] M. Amati, M. Tomasetti, M. Scartozzi, L. Mariotti, R. Alleva, E. Pignotti, B. Borghi, M. Valentino, M. Governa, J. Neuzil, L. Santarelli, Profiling tumor-associated markers for early detection of malignant mesothelioma: an epidemiologic study Cancer Epidemiol, Biomarkers Prev 17 (2008) 163–170.

[22] K. Schelch, M.B. Kirschner, M. Williams, Y.Y. Cheng, N. van Zandwijk, M. Grusch, G. Reid, A link between the fibroblast growth factor axis and the miR-16 family reveals potential new treatment combinations in mesothelioma, Mol. Oncol. 12 (2018) 58–73.

[23] Z. Benyahia, N. Dussault, M. Cayol, R. Sigaud, C. Berenguer-Daizé, C. Delfino, A. Tounsi, S. Garcia, P.M. Martin, K. Mabrouk, L. Ouafik, Stromal fibroblasts present in breast carcinomas promote tumor growth and angiogenesis through adrenomedullin secretion, Oncotarget 8 (2017) 15744–15762.

[24] T.H. Huang, T.Y. Chu, Repression of miR-126 and upregulation of adrenomedullin in the stromal endothelium by cancer-stromal cross talks confers angiogenesis of cervical cancer, Oncogene 33 (2014) 3636–3647.

[25] J. He, X. Qian, R. Carpenter, Q. Xu, L. Wang, Y. Qi, Z.X. Wang, L.Z. Liu, B.H. Jiang, Repression of miR-143 mediates Cr (VI)-induced tumor angiogenesis via IGF-IR/IRS1/ERK/IL-8 pathway, Toxicol. Sci. 134 (2013) 26–38.

[26] A. Salajegheh, Insulin Receptor Substrate (IRS-1). Angiogenesis in Health, Disease and Malignancy, Springer, Cham, 2016, pp. 189–192.

[27] Y. Wang, X. Zhang, C. Zou, H.F. Kung, M.C. Lin, A. Dress, F. Wardle, B.H. Jiang, L. Lai, miR-195 Inhibits Tumor Growth and Angiogenesis through Modulating IRS1 in Breast Cancer Biomed Pharmacother vol. 80, (2016), pp. 95–101.

[28] C.D. Hoang, X. Zhang, P.D. Scott, T.J. Guillaume, M.A. Maddaus, D. Yee, R.A. Kratzke, Selective activation of insulin receptor substrate-1 and -2 in pleural mesothelioma cells: association with distinct malignant phenotypes, Cancer Res. 64 (2004) 7479–7485.
[29] E.K. Kim, E.J. Choi, Pathological roles of MAPK signaling pathways in human diseases, Biochim. Biophys. Acta 1802 (2010) 396–405.
[30] M. Ye, Q. Ni, H. Qi, X. Qian, J. Chen, X. Guo, M. Li, Y. Zhao, G. Xue, H. Deng, L. Zhang, Exosomes derived from human induced pluripotent stem cells-endothelia cells promotes postnatal angiogenesis in mice bearing ischemic limbs, Int. J. Biol. Sci. 15 (2019) 158–168.
[31] Y. Jiang, H. Xie, W. Tu, H. Fang, C. Ji, T. Yan, H. Huang, C. Yu, Q. Hu, Z. Gao, S. Lv, Exosomes secreted by HUVECs attenuate hypoxia/reoxygenation-induced apoptosis in neural cells by suppressing miR-21-3p, Am. J. Transl. Res. 10 (2018) 3529–3541.
[32] J. Sun, Z. Zhang, T. Ma, Z. Yang, J. Zhang, X. Liu, D. Lu, Z. Shen, J. Yang, Q. Meng, Endothelial progenitor cell-derived exosomes, loaded with miR-126, promoted deep vein thrombosis resolution and recanalization, Stem Cell Res. Ther. 9 (2018) 223.